

Available online at www.synsint.com

Synthesis and Sintering

ISSN 2564-0186 (Print), ISSN 2564-0194 (Online)



Research article

Electrochemical evaluation of the hydroxyapatite coating synthesized on the AZ91 by electrophoretic deposition route



Arezoo Jangjoo Tazeh Kand ^a, Fereshteh Afaghi ^a, Arvin Taghizadeh Tabrizi ^b, Hossein Aghajani ^{b,*}, Hilal Demir Kivrak ^c

^a Materials Engineering Department, University of Tabriz, Tabriz, Iran

^b School of Metallurgy and Materials Engineering, Iran University of Science and Technology, Narmak, Tehran, Iran

^c Department of Chemical Engineering, Faculty of Engineering and Architectural Sciences, Eskisehir Osmangazi University, Eskisehir, Turkey

ABSTRACT

The hydroxyapatite layer was deposited on the commercial magnesium alloy of AZ91 by electrophoretic deposition route, and the corrosion behavior of applied layers was studied by polarization and electrochemical impedance spectroscopy at the Simulated Body Fluid (SBF) solution. The best corrosion resistance improvement was obtained for the sample synthesized at 40 V within 4 minutes. Also, the morphology of coated samples was studied by atomic force microscopy (AFM) and the surface parameters were measured. It could be concluded that the calculated values for surface parameters including surface roughness, maximum peak height, maximum pit depth, and maximum peak have a meaningful relationship with corrosion resistance.

© 2021 The Authors. Published by Synsint Research Group.

KEYWORDS

Hydroxyapatite layer
Magnesium alloy
Electrophoretic deposition
Electrochemical impedance spectroscopy
Synthesis



1. Introduction

Bioengineering is one of the new engineering fields which attract great attention among researchers. One of the most critical issues in this field is materials that could be used in a human's body, called biomaterials [1]. Generally, all engineering materials, including glasses [2], ceramics, metals, and polymers could be used in a human's body [3]. Used Biomaterials should be composed of two important features including biocompatibility and nontoxicity. Many metals are known as biomaterials including titanium, 316 stainless steel [4], cobalt alloys [5], and magnesium alloys [6]. Despite the exclusive properties offered by metal-based biomaterials like higher strength, their main drawback is low corrosion resistance. The main solution to overcome this problem is applying corrosion-resistant coating on the surface of the substrates [7]. The magnesium alloys show a combination of exclusive properties especially the light weight but the main drawback is their poor corrosion resistance.

Among different inorganic materials like carbon nanotubes, bioactive glasses, calcium phosphate, chitosan, gelatin, and silk fibroin, hydroxyapatite is the most similar material to the chemical composition of bone [8, 9]. Therefore, it is the best candidate to apply as a coating on the substrates to increase the adhesion of the metallic implants, and many investigations have been done before to investigate the applied hydroxyapatite coatings [10]. Patel et al. [11] reported the coating of titanium by three different hydroxyapatites with diverse morphology and obtained dense and uniform coating. Among all deposition methods, it is mentioned in the literature that electrophoretic deposition has a better influence than other methods like plasma spray [12]. There are many investigations that have been conducted before on applying the hydroxyapatite layer on a different substrate like Si [13] titanium alloys [14, 15] especially on NiTi [16, 17] and 316L stainless steel [18, 19], but there are rare investigations done on magnesium alloy [20, 21]. AZ91 is introduced as newly developed in bio and medical applications due to its unique properties like low density. But

* Corresponding author. E-mail address: haghajani@iust.ac.ir (H. Aghajani)

Received 18 May 2021; Received in revised form 1 June 2021; Accepted 4 June 2021.

Peer review under responsibility of Synsint Research Group. This is an open access article under the CC BY license (<https://creativecommons.org/licenses/by/4.0/>).
<https://doi.org/10.53063/synsint.2021.1226>

for broadening its application, the low corrosion resistance of AZ91 must be improved. Applying HA layer could improve this feature of AZ91. Singh et al. [22] investigated the corrosion behavior of HA composite coating on AZ91 by polarization and immersion routes before and reported that HA coatings improve the corrosion resistance. In this paper, electrochemical impedance spectroscopy was performed on the hydroxyapatite layers.

2. Experiments

2.1. Suspension preparation

The suspensions for EPD were prepared using solid iodine (as a stabilizer and increasing the surface charge of hydroxyapatite), triethanolamine, TEA (as a dispersant) [23], and commercially available hydroxyapatite nanoparticles (particle size of 10–15 nm) in the concentration of 1 wt%. The suspensions were magnetically stirred for 30 min followed by 15 min ultra-sonication.

2.2. EPD coating process

The Mg-alloy, AZ91, substrates used as electrodes were planar cut in dimension $40 \times 10 \times 3$ mm. The electrodes are separated by a distance of 16 mm in the EPD cell. Before EPD, the surface treatment was applied on substrate respectively grinding 80–2000 mesh with SiC papers, polished, and washed in deionized water for 10 min. Subsequently degreased with acetone bath ultrasonically and rinsed with distilled water and dried in air. Different peak-to-peak voltages from 4 to 6 V and times from 4 to 6 minutes were considered to obtain electrophoretic coatings. It should be noted that there is no agitation in the EPD cell during the coating process. Also, the schematic of the EPD process is shown in Fig. 1. After coating, the samples are kept at room temperature for 24 hours. The codification of samples is presented in Table 1.

2.3. Characterization

Surface morphology studies were conducted by using a field emission scanning electron microscope. Also, the surface morphology of samples and average surface roughness were determined using none contact mode of atomic force microscopy (AFM, Nanosurf Mobile S Model, Nanosurf Company, Switzerland) equipped with a Dual Scopes C-21 controller, a DS-95-200-E scanner, and Si_3N_4 needle. The scanning rate and applied load on the needle tip were 24 $\mu\text{m/s}$ and 0.15 nN, respectively, and the surface parameters were calculated by open-source software, Gwyddion (version 2.59).

Electrochemical polarization experiment was carried out using an Auto-Lab Corrosion measurement system. Electrodes (Saturated calomel (KCl), platinum & coated/un-coated sample) for this aim were arranged by connecting a copper wire to one side of the samples and masked with cold setting resin and the opposite surface of the specimens (1 cm^2) was subjected to the solution. The specimens were offered a metallographic polishing before each experiment, followed by a wash with distilled water and acetone. A polarization test was performed in a corrosion cell having 250 ml of 3.5% SBF using a standard three-electrode configuration. Specimens were submerged in the analysis solution and a polarization scan was adjusted towards more noble values at a rate of $0.5 \text{ mV} \cdot \text{s}^{-1}$, in the range of -20 to 520 mV, after allowing a steady-state potential to develop after 30 min.

Table 1. Sample codification.

Sample	Voltage (V)	Time (min)
HA-304	30	4
HA-306	30	6
HA-404	40	4
HA-406	40	6

3. Results and discussion

The weight gained during EPD by varying deposition time and applied voltage at constant voltage and constant deposition time was measured and depicted in Fig. 2 to evaluate the rate of deposition. It is shown that the deposition rate has a direct linear relation with deposition parameters like applied voltage and deposition duration, but the slopes are different. According to Fig. 2a, it is shown that by increasing the time of deposition, more hydroxyapatite was deposited on the surface of the substrates. Also, the effect of the applied voltage on the weight of the obtained layer is shown in Fig. 2b where it is exhibited that by increasing the applied voltage, more hydroxyapatite was deposited on the surface. According to Fig. 2b, by increasing the applied voltage of the deposition, the amount of hydroxyapatite on the AZ91 surface decreased. It could be due to the surface charge of the hydroxyapatite particles suspended in the deposition solution.

The morphologies of applied hydroxyapatite layers on AZ91 are displayed in Fig. 3. It is shown that the uniform layer had been obtained on the surface of the samples, presented in FE-SEM images of Figs. 3c, 3e, and 3g. Some porosity is seen on the surface of the sample HA-304, Fig. 3a. At higher magnifications presented in Figs. 3b, 3d, 3f, and 3h it can be seen that the morphology of the deposited hydroxyapatite differs from various deposition times and applied voltages. According to these FE-SEM images, achieved morphology in all samples is sponge-like morphology but in samples, HA-304 and HA-404 it is agglomerated and the shape of the particles is more similar to a sphere, but in the samples, HA-306 and HA-406, the obtained morphology of the hydroxyapatite particles looks like a rod. It could be declared that by increasing the deposition time, more rod

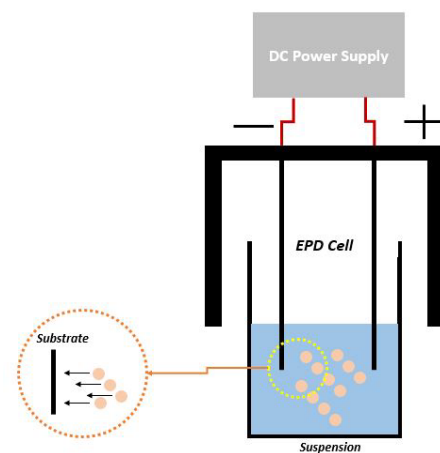


Fig. 1. The schematic of EPD cell.

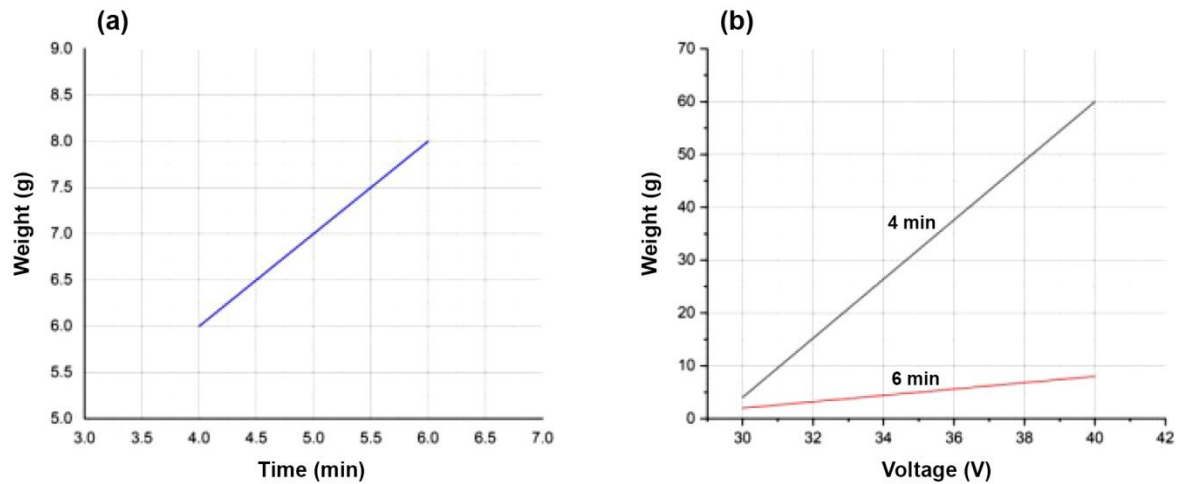


Fig. 2. The effect of time and applied voltage on the amount of deposited hydroxyapatite, a) constant voltage of 30 V, b) constant time of 4 and 6 min.

morphology of the hydroxyapatite particles was formed, which was due to the kinetic aspect of the deposition process. Also, some porosity could be seen in Figs. 3b, 3f, and 3h.

The polarization curves of the samples are presented in Fig. 4. No passive behavior was observed in any sample. The improvement in corrosion resistance was seen in the polarization curve of sample HA-404. This could be due to a more uniform layer deposited in this sample. Due to the good linear behavior of the coatings, the corrosion parameters including corrosion current density, i_{corr} , corrosion potential, E_{corr} , and corrosion resistance, R_p , are calculated by Tafel extrapolation and are displayed in Table 2. It is shown that by applying the hydroxyapatite layer on the surface of the AZ91 substrate, the corrosion current density increased and the maximum value was obtained in sample HA-306, but the minimum value obtained in sample

HA-406 equals 0.05 A/cm^2 , which is lower than the base metal. Also, the corrosion potential shifted to more positive values by applying the hydroxyapatite layer. The maximum value obtained in sample HA-404 equals -0.001 V . The corrosion resistance was calculated based on the Stern-Gary equation and the maximum corrosion resistance obtained in sample HA-404 equals 37.7 ohms and the minimum one achieved in sample HA-306 equals 0.7 ohms . Regarding the calculated values for corrosion resistance, it could be declared that only applying the hydroxyapatite in the optimum condition of 40 voltages within 4 minutes improves the corrosion resistance. This might be due to the shape of hydroxyapatite particles deposited in this condition which was reported before by Goudarzi et al. [25] by studying the corrosion behavior of hydroxyapatite coatings on anodized nano-tubular TiO_2 structures. Other achieved layers cause a decrease in corrosion

Table 2. Calculated corrosion parameters achieved from polarization curve.

Sample	$I_{\text{corr}} \text{ (A/cm}^2\text{)}$	$E_{\text{corr}} \text{ (V)}$	$R_p \text{ (ohm)}$
AZ91	0.1202	-1.33	3.7
HA-304	0.1620	-1.26	2.6
HA-404	0.1563	-0.001	37.7
HA-306	2.8	-1.5	0.7
HA-406	0.058	-1.1	1.9

Table 3. Calculated values for impedance parameters by Zview software.

Sample	$R_s \text{ (ohm)}$	$C_{\text{coat-T}} \text{ (F)}$	$C_{\text{coat-P}} \text{ (F)}$	$R_{\text{coat}} \text{ (ohm)}$	$R_{\text{corr}} \text{ (ohm)}$	$L \text{ (H)}$
AZ91	41.23	1.61E-5	0.887	339	483.4	47.92
HA-304	38.37	1.20E-5	0.93	87.93	264.9	12.76
HA-404	39.67	1.31E-5	0.89	111.9	650.2	11.53
HA-306	48.82	2.12E-5	0.889	56.9	102.6	5.071
HA-406	39.73	1.40E-5	0.9	149.6	188.1	25.7

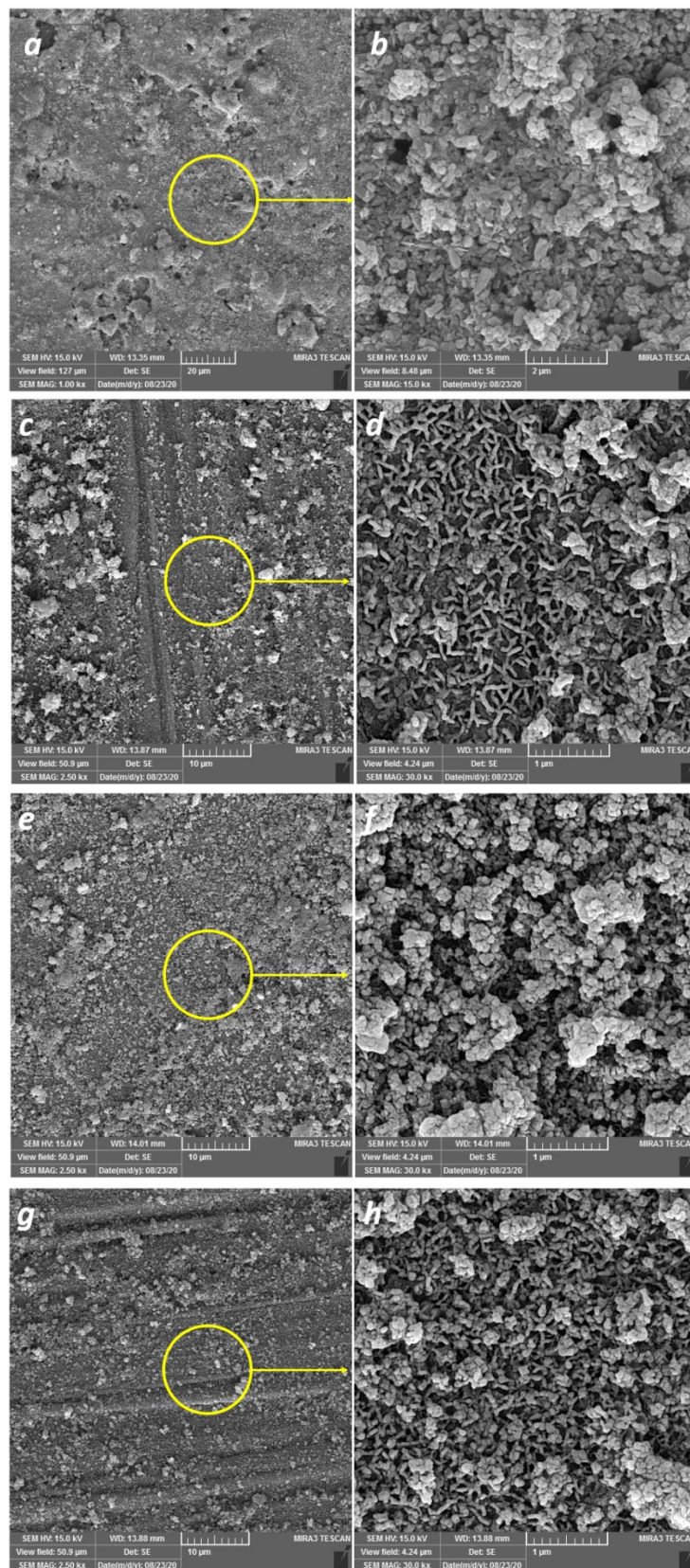


Fig. 3. FE-SEM images of the morphologies of a, b) HA-304, c, d) HA-404, e, f) HA-306, and g, h) HA-406

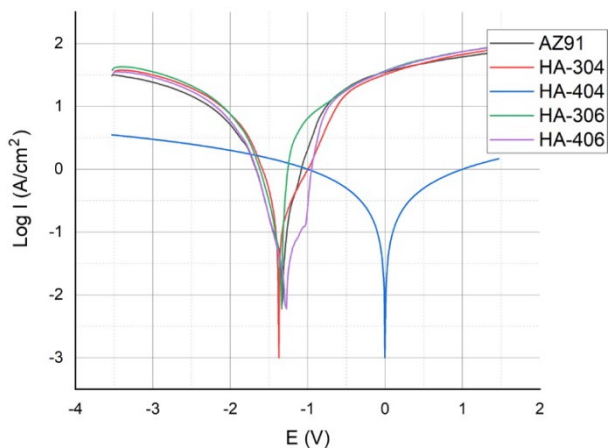


Fig. 4. Polarization curves achieved from polarization test in 3.5 wt% SBF solution.

resistance. Also, the formation of the micro pore-free layer on the surface of the substrate acts as an effective barrier in the penetration of corrosive agents and improves corrosion resistance.

For a detailed study of the corrosion behavior, electrochemical impedance spectroscopy (EIS) was performed on the deposited hydroxyapatite layers. The fitted Nyquist curves are presented in Fig. 5. The obtained results are in good conformity with the results of the polarization test. These plots are used to describe the important impedance parameters including resistance and capacitance of the electrochemical system, where contains the applied coating on the substrate. It is shown in Fig. 5 that all samples have two parts on the Nyquist curves, the first part represents the effect of the hydroxyapatite layer at higher frequencies and the second part displays an inductive behavior where the Nyquist plots are negative at low frequencies attributed to the localized corrosion occurred on the surface of the deposited hydroxyapatite layer. The presented equivalent circuit in this figure which includes three resistances, one capacitor, and one inductor, has well fitted, from the mathematical aspect of view. Finally, the impedance parameters based on the proposed equivalent circuit

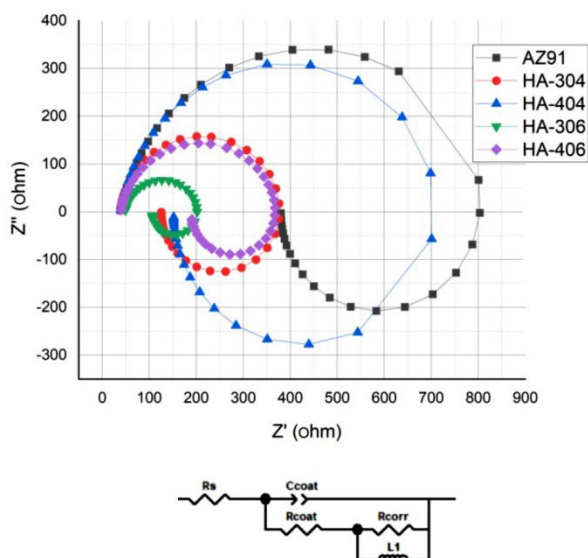


Fig. 5. Fitted Nyquist plots for deposited samples.

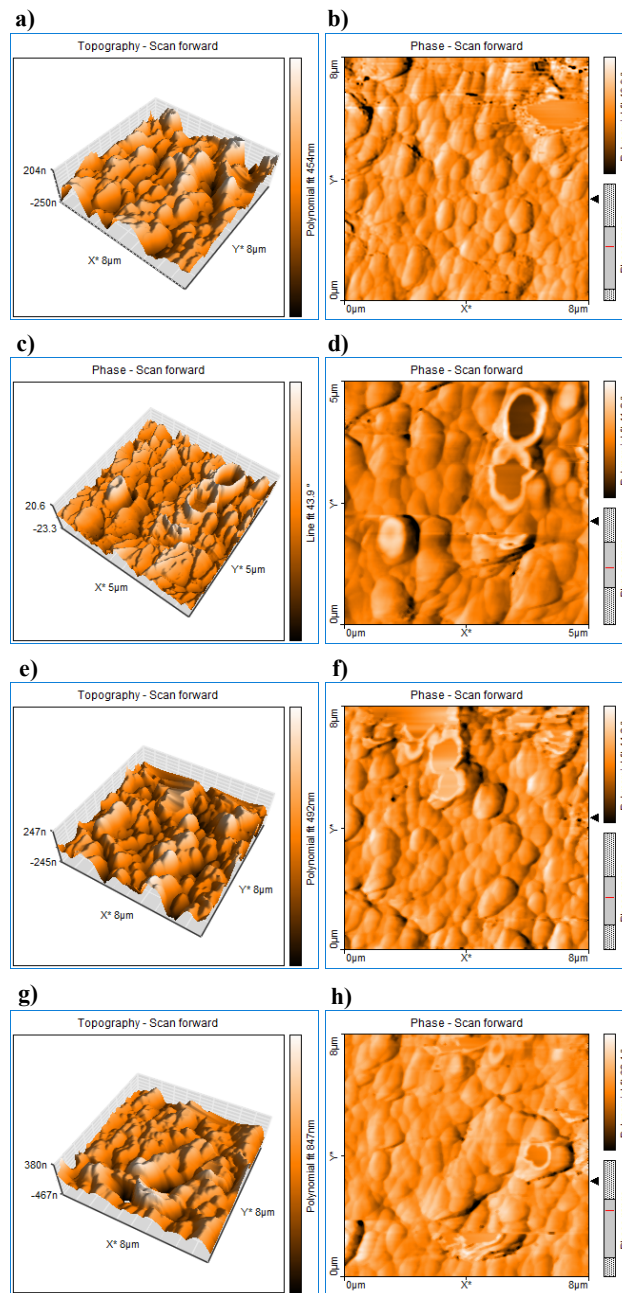


Fig. 6. AFM 3D and 2D plots of a, b) HA-304, c, d) HA-404, e, f) HA-306, and g, h) HA-406.

were calculated through Zview software, and results are presented in Table 3 where sample HA-404 shows the best corrosion resistance.

Farnoush et al. [26] proposed the corrosion mechanism for HA-TiO₂ composite coatings. In this mechanism, Ca²⁺ and PO₄⁴⁻ ions are released into the corrosive SBF solution by exchanging H₃O⁺ ions to form Ti-OH groups on the surface. Therefore, here, it could be declared that the formation of Mg-OH groups on the surface occurred and caused the ion activity in the solution. The Mg-OH causes the formation of positive ions in the solution as below:



The 3D plots of surface morphology achieved by atomic force microscopy are presented in Fig. 6. The morphologies of the deposited

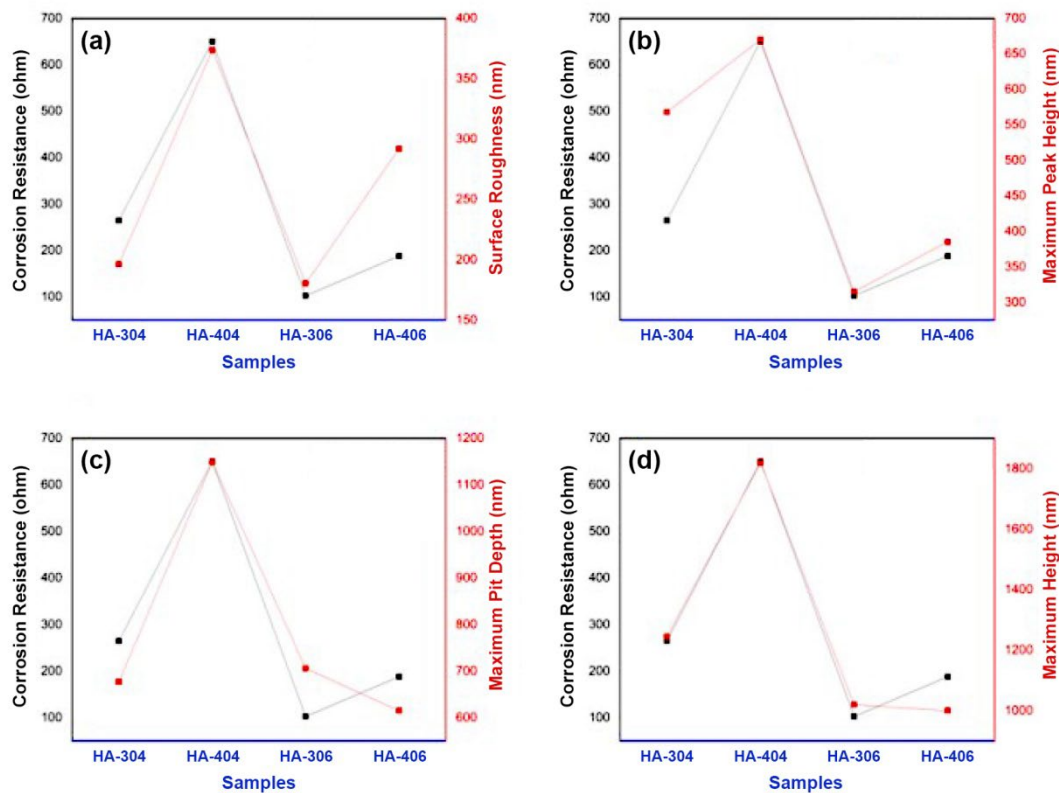


Fig. 7. Plotted diagrams of corrosion resistance and surface parameters, a) Sa, b) Sp, c) Sv, and d) Sz.

layers are obvious that almost all sphere particles are deposited on the surface of the AZ91 substrate. The surface parameters of deposited hydroxyapatite layers are presented in Table 4. It is worthy to note that Sa, Sp, Sv, and Sz represent surface roughness, maximum peak height, maximum pit depth, and maximum peak respectively. It is shown that maximum values for these surface parameters have been obtained in sample HA-404 which showed better corrosion resistance. The values measured for the samples HA-404 and HA-406 which consist of rod shape morphology have higher surface roughness and they are in the range that Singh et al. [22] reported before. Then it could be concluded that the calculated values for these parameters have a meaningful relationship with corrosion resistance. The plotted diagrams in Fig. 7 confirm this claim and show the same fluctuation in corrosion resistance and surface parameters. The diagrams show that variation of Sa and Sp has better relation with measured corrosion resistance. Also, it is obvious that sample with higher corrosion resistance, has higher values of surface parameters for Sa, Sp, Sv and Sz equaling 373.3, 670, 1149, and 1245 nm, repetitively.

Table 4. Calculated surface parameters from AFM results.

Sample	Sa (nm)	Sp (nm)	Sv (nm)	Sz (nm)
HA-304	196.3	568	677	1245
HA-404	373.7	670	1149	1819
HA-306	180.6	315	706	1020
HA-406	291.9	385.2	614.8	1000

4. Conclusions

The corrosion behavior of the hydroxyapatite layer which is deposited by the electrophoretic deposition route was studied by polarization and electrochemical impedance spectroscopy (EIS). Results show that the layer which was synthesized at 40 V within 4 minutes has an improvement in corrosion resistance. This improvement has a meaningful relationship with calculated values of surface parameters obtained from atomic force microscopy (AFM), which shows that the maximum values of surface roughness, maximum peak height, maximum peak, and maximum pit depth have better corrosion resistance.

CRediT authorship contribution statement

Arezoo Jangjoo Tazeh Kand: Formal Analysis, Investigation, Methodology.

Fereshteh Afaghi: Formal Analysis, Investigation, Methodology.

Arvin Taghizadeh Tabrizi: Methodology, Conceptualization, Writing – review & editing.

Hossein Aghajani: Supervision, Conceptualization, Writing-Original Draft.

Hilal Demir Kivrak: Methodology, Formal Analysis.

Data availability

The data underlying this article will be shared on reasonable request to the corresponding author.

Declaration of competing interest

The authors declare no competing interests.

Funding and acknowledgment

The authors express their gratitude to the University of Tabriz for their generous financial support and for providing the necessary instruments and equipment essential for the successful completion of this study.

References

- [1] M. Ding, N. Sahebgharani, F. Musharavati, F. Jaber, E. Zalnezhad, G.H. Yoon, Synthesis and properties of HA/ZnO/CNT nanocomposite, *Ceram. Int.* 44 (2018) 7746–7753. <https://doi.org/10.1016/j.ceramint.2018.01.203>.
- [2] M. Ji, H. Li, H. Guo, A. Xie, S. Wang, et al., A novel porous aspirin-loaded (GO/CTS-HA)_n nanocomposite films: Synthesis and multifunction for bone tissue engineering, *Carbohydr. Polym.* 153 (2016) 124–132. <https://doi.org/10.1016/j.carbpol.2016.07.078>.
- [3] C. Prakash, S. Singh, K. Verma, S.S. Sidhu, S. Singh, Synthesis and characterization of Mg-Zn-Mn-HA composite by spark plasma sintering process for orthopedic applications, *Vacuum*. 155 (2018) 578–584. <https://doi.org/10.1016/j.vacuum.2018.06.063>.
- [4] Z.M. Al-Rashidy, M.M. Farag, N.A. Abdel Ghany, A.M. Ibrahim, W.I. Abdel-Fattah, Orthopaedic bioactive glass/chitosan composites coated 316L stainless steel by green electrophoretic co-deposition, *Surf. Coat. Technol.* 334 (2018) 479–490. <https://doi.org/10.1016/j.surfcoat.2017.11.052>.
- [5] T. Moskalewicz, A. Lukaszczyk, A. Kurk, M. Kot, D. Jugowicz, et al., Porous HA and nanocomposite nc-TiO₂/HA coatings to improve the electrochemical corrosion resistance of the Co-28Cr-5Mo alloy, *Mater. Chem. Phys.* 199 (2017) 144–158. <https://doi.org/10.1016/j.matchemphys.2017.06.064>.
- [6] A. Bordbar Khiabani, S. Rahimi, B. Yarmand, M. Mozafari, Electrophoretic deposition of graphene oxide on plasma electrolytic oxidized-magnesium implants for bone tissue engineering applications, *Mater. Today Proc.* 5 (2018) 15603–15612. <https://doi.org/10.1016/j.matpr.2018.04.169>.
- [7] S.A. Naziri Mehrabani, R. Ahmadzadeh, N. Abdian, A. Taghizadeh Tabrizi, H. Aghajani, Synthesis of Ni-GO nanocomposite coatings: Corrosion evaluation, *Surf. Interfaces*. 20 (2020) 100546. <https://doi.org/10.1016/j.surfint.2020.100546>.
- [8] A. Pawlik, M.A.U. Rehman, Q. Nawaz, F.E. Bastan, G.D. Sulka, A.R. Boccaccini, Fabrication and characterization of electrophoretically deposited chitosan-hydroxyapatite composite coatings on anodic titanium dioxide layers, *Electrochim. Acta*. 307 (2019) 465–473. <https://doi.org/10.1016/j.electacta.2019.03.195>.
- [9] S. Koesnarjadi, S.J. Santosa, D. Siswanta, B. Rusdiarso, Synthesis and Characterization of Magnetite Nanoparticle Coated Humic Acid (Fe₃O₄/HA), *Procedia Environ. Sci.* 30 (2015) 103–108. <https://doi.org/10.1016/j.proenv.2015.10.018>.
- [10] S. Türk, I. Altınsoy, G.Ç. Efe, M. Ipek, M. Özacar, C. Bindal, Biomimetic synthesis of Ag, Zn or Co doped HA and coating of Ag, Zn or Co doped HA/fMWCNT composite on functionalized Ti, *Mater. Sci. Eng. C*. 99 (2019) 986–998. <https://doi.org/10.1016/j.msec.2019.02.025>.
- [11] K.D. Patel, R.K. Singh, J.H. Lee, H.W. Kim, Electrophoretic coatings of hydroxyapatite with various nanocrystal shapes, *Mater. Lett.* 234 (2019) 148–154. <https://doi.org/10.1016/j.matlet.2018.09.066>.
- [12] O.S. Yildirim, B. Aksakal, H. Celik, Y. Vangolu, A. Okur, An investigation of the effects of hydroxyapatite coatings on the fixation strength of cortical screws, *Med. Eng. Phys.* 27 (2005) 221–228. <https://doi.org/10.1016/j.medengphy.2004.10.006>.
- [13] A. Clifford, X. Pang, I. Zhitomirsky, Biomimetically modified chitosan for electrophoretic deposition of composites, *Colloids Surf.* 544 (2018) 28–34. <https://doi.org/10.1016/j.colsurfa.2018.02.028>.
- [14] D. Jugowicz, A. Lukaszczyk, L. Cieniek, K. Kowalski, L. Rumian, et al., Influence of the electrophoretic deposition route on the microstructure and properties of nano-hydroxyapatite/chitosan coatings on the Ti-13Nb-13Zr alloy, *Surf. Coat. Technol.* 324 (2017) 64–79. <https://doi.org/10.1016/j.surfcoat.2017.05.056>.
- [15] M. Bartmanski, B. Cieslik, J. Glodowska, P. Kalka, L. Pawlowski, et al., Electrophoretic deposition (EPD) of nanohydroxyapatite - nanosilver coatings on Ti13Zr13Nb alloy, *Ceram. Int.* 43 (2017) 11820–11829. <https://doi.org/10.1016/j.ceramint.2017.06.026>.
- [16] F.E. Baştan, M. Atiq Ur Rehman, Y.Y. Avcu, E. Avcu, F. Üstel, A.R. Boccaccini, Electrophoretic co-deposition of PEEK-hydroxyapatite composite coatings for biomedical applications, *Colloids Surf. B*. 169 (2018) 176–182. <https://doi.org/10.1016/j.colsurfb.2018.05.005>.
- [17] V. Khalili, J. Khalil-Allafi, C. Sengstock, Y. Motemani, A. Paulsen, et al., Characterization of mechanical properties of hydroxyapatite-silicon-multi walled carbon nano tubes composite coatings synthesized by EPD on NiTi alloys for biomedical application, *J. Mech. Behav. Biomed. Mater.* 59 (2016) 337–352. <https://doi.org/10.1016/j.jmbbm.2016.02.007>.
- [18] S. Mahmoodi, L. Sorkhi, M. Farrokhi-Rad, T. Shahrabi, Electrophoretic deposition of hydroxyapatite-chitosan nanocomposite coatings in different alcohols, *Surf. Coat. Technol.* 216 (2013) 106–114. <https://doi.org/10.1016/j.surfcoat.2012.11.032>.
- [19] M. Farrokhi-Rad, Electrophoretic deposition of hydroxyapatite fiber reinforced hydroxyapatite matrix nanocomposite coatings, *Surf. Coat. Technol.* 329 (2017) 155–162. <https://doi.org/10.1016/j.surfcoat.2017.09.051>.
- [20] Q. Tayyaba, M. Shahzad, A.Q. Butt, Rafi-ud-din, M. Khan, A.H. Qureshi, The influence of electrophoretic deposition of HA on Mg-Zn-Zr alloy on its in-vitro degradation behaviour in the Ringer's solution, *Surf. Coat. Technol.* 375 (2019) 197–204. <https://doi.org/10.1016/j.surfcoat.2019.07.014>.
- [21] M. Razavi, M. Fathi, O. Savabi, D. Vashae, L. Tayebi, In vivo assessments of bioabsorbable AZ91 magnesium implants coated with nanostructured fluoridated hydroxyapatite by MAO/EPD technique for biomedical applications, *Mater. Sci. Eng. C*. 48 (2015) 21–27. <https://doi.org/10.1016/j.msec.2014.11.020>.
- [22] S. Singh, G. Singh, N. Bala, Corrosion behavior and characterization of HA/Fe₃O₄/CS composite coatings on AZ91 Mg alloy by electrophoretic deposition, *Mater. Chem. Phys.* 237 (2019) 121884. <https://doi.org/10.1016/j.matchemphys.2019.121884>.
- [23] S. Khanmohammadi, M. Ojaghi-Ilkchi, M. Farrokhi-Rad, Evaluation of Bioglass and Hydroxyapatite Based Nanocomposite Coatings Obtained by Electrophoretic Deposition, *Ceram. Int.* 46 (2020) 26069–26077. <https://doi.org/10.1016/j.ceramint.2020.07.100>.
- [24] E. Avcu, F.E. Baştan, H.Z. Abdullah, M.A.U. Rehman, Y.Y. Avcu, A.R. Boccaccini, Electrophoretic deposition of chitosan-based composite coatings for biomedical applications: A review, *Prog. Mater. Sci.* 103 (2019) 69–108. <https://doi.org/10.1016/j.pmatsci.2019.01.001>.
- [25] M. Goudarzi, F. Batmanghelich, A. Afshar, A. Dolati, G. Mortazavi, Development of electrophoretically deposited hydroxyapatite coatings on anodized nanotubular TiO₂ structures: Corrosion and sintering temperature, *Appl. Surf. Sci.* 301 (2014) 250–257. <https://doi.org/10.1016/j.apsusc.2014.02.055>.
- [26] H. Farnoush, G. Aldiç, H. Çimenöglü, Functionally graded HA-TiO₂ nanostructured composite coating on Ti-6Al-4V substrate via electrophoretic deposition, *Surf. Coat. Technol.* 265 (2015) 7–15. <https://doi.org/10.1016/j.surfcoat.2015.01.069>.